第 49 卷第 8 期
2021 年 8 月

硅 酸 盐 学 报
JOURNAL OF THE CHINESE CERAMIC SOCIETY

Vol. 49，No. 8
August，2021

http://www.gxyb.cbpt.cnki.net

DOI：10.14062/j.issn.0454-5648.20200868

氧化铝添加对硼硅酸盐结构和化学耐久性的影响

MOHAMED A Ali[1]，刘小峰[2]，邱建荣[1]

(1. 浙江大学现代光学仪器国家重点实验室，浙江大学光电科学与工程学院，杭州 310027；
2. 浙江大学材料科学与工程学院，杭州 310027)

摘　要：通过耐液性试验，研究了添加 Al_2O_3 对硼硅酸盐玻璃[$70SiO_2$–$(20–x)B_2O_3$–xAl_2O_3–$10Na_2O$，x=0、5、10、15、20，摩尔分数]的抗水、盐酸和氢氧化钠水溶液腐蚀性能的影响，讨论了铝硅酸盐玻璃在不同化学结构下的化学侵蚀机理。结果表明：在氧化玻璃网络中加入 Al^{3+}后，该玻璃在水、HCl 和 NaOH 水溶液中的化学耐久性显著提高；不含 Al_2O_3 的玻璃化学耐久性较差与熔融玻璃中存在含 3 个和 4 个非桥氧(NBO)的 BO_4 有关，在水溶液侵蚀后，玻璃被更快地侵蚀，形成多孔玻璃表面。在非晶态玻璃网络中添加 Al_2O_3，抑制了 BO_4 的生成，提高了材料的化学耐久性。

关键词：化学耐久性；玻璃；氧化铝；结构；硼硅酸盐
中图分类号：TQ171.1　　**文献标志码**：A　　**文章编号**：0454–5648(2021)08–1527–16
网络出版时间：2021–07–15

Effect of Alumina on Structure and Chemical Durability of Borosilicate Glasses

MOHAMED A Ali[1], LIU Xiaofeng[2], QIU Jianrong[1]

(1. State Key Laboratory of Modern Optical Instrumentation, College of Optical Science and Engineering, Zhejiang University, Hangzhou 310027, China; 2. School of Materials Science and Engineering, Zhejiang University, Hangzhou 310027, China)

Abstract: The effect of alumina (Al_2O_3) on the chemical durability of borosilicate glasses, $70SiO_2$–$(20–x)B_2O_3$–xAl_2O_3–$10Na_2O$, x=0, 5, 10, 15 and 20 (molar fraction), in water, HCl and NaOH aqueous solutions, was investigated *via* liquid resistance tests. The chemical stability of aluminoborosilicate glass was discussed based on the glass structure, and the mechanism of chemical attack in different solutions was proposed. The results show that a significant enhancement in the chemical durability in water, HCl and NaOH aqueous solutions occurs after the incorporation of Al^{3+} into the oxide glass network. The structural analysis indicates that the relatively low chemical durability of the glass as x=0 is correlated to the presence of BO_4 with three and four non-bridging oxygen (NBO) in the melts. Consequently, the glass is eroded more quickly during the attack of the aqueous solutions, resulting in a porous glass surface. The chemical durability can be improved due to the addition of Al_2O_3 into the glass network, suppressing the formation of BO_4.

Keywords: chemical durability; glass; alumina; strucutre; borosilicate

1 Introduction

Chemical durability of glass is one of the properties that reflects the ability of glass to resist the corrosion against water and various aqueous solutions of acids or alkalis[1]. High chemical stability of glass is needed to enable the practical applications of glasses in some applications including medicine, nuclear waste treatment, optoelectronics, *etc.*[2–6]. The glass resistance to chemical solutions relies on several factors, such as glass composition, structure and surface state as well as solution type and exposure temperature and time, *etc.*[7–10]. If silicate glass contains alkali or other highly mobile ions, chemical attack in an aqueous solution on glass causes a corrosion on glass surface as a result of various chemical reactions[11].

收稿日期：2020–11–19。　修订日期：2020–12–23。
基金项目：国家重点研发计划项目(2018YFB1107200)；国家自然科学基金项目(52050410326，51772270，617751)。
第一作者：Mohamed A Ali (1987–)，博士。
通信作者：邱建荣(1964—)，男，博士，教授。

Received date: 2020–11–19.　**Revised date:** 2020–12–23.
First author: MOHAMED A Ali (1987–), Ph. D..
E-mail: mohamedali@zju.edu.cn
Correspondent author: QIU Jianrong (1964–), male, Ph. D., Professor.
E-mail: qjr@zju.edu.cn

In general, glass is more chemically stable than most metals and polymers[12–14]. However, many non-silicate glasses such as phosphates and borates can be dissolved in aqueous acid solutions[15–16]. Moreover, glasses with a good chemical durability under ambient conditions are slowly dissolved if they are exposed to strong aqueous acid or alkali solutions at high temperatures[17–18]. In glass industry, commercial borosilicate glass containing alkali oxides is widely used in various applications. Currently, borosilicate glass bottles are used to store medicine in the field of pharmacy. These glasses possess a good chemical durability against aqueous solutions, while medicine storage for long periods reduces the stability of glass, leading to the dissolution of some glass compositions *e.g.,* alkali ions into medicament. Several methods have been used to enhance the chemical durability of glass, such as, (i) increasing silica and/or alumina content to reduce the mobility of alkali ions, (ii) decreasing the content of alkali ions on the surface and (iii) coating some films on the glass surface that serves as a barrier between the fluid and glass[19]. Most previous reports attempted to improve the chemical durability of glasses against different aqueous solutions by adjusting the glass composition and heat treatment condition[15–18,20–21]. However, the local structural differences of glasses before and after attack in aqueous solutions has been rarely investigated in details.

In this study, we investigated the chemical stability of borosilicate glass in water, NaOH or HCl aqueous solutions by adding Al_2O_3 into the glass to modify glass network structure. In addition, the relationship between the chemical durability and glass composition and the coresponding corrosion mechanism on the glasses surface were also discussed.

2 Experimental

2.1 Preparation

Aluminoborosilicate glasses $70SiO_2$-$(20–x)B_2O_3$-xAl_2O_3-$10Na_2O$ (mole fraction, %), x=0, 5, 10, 15 and 20 were prepared by a conventional melt-quenching method. For each batch, approximately 500 g of starting material (*i.e*., SiO_2, H_3BO_3, Al_2O_3 and Na_2CO_3) was fully mixed in a mechanical grinding mixer for 20 min. A small amount of SnO_2 (0.2%) was used as a fining agent. For glass samples with x=0 and 5, the batches were melted at 1 450 ℃ for 1 h and stirred for additional 1 h, and then at 1 500 ℃ for 2 h. For glass samples with x=10, 15 and 20, the batches were melted at 1 600 ℃ for 1 h under constant stirring for 20 min and finally at 1 680 ℃ for 4 h. All the batches were melted in a Pt/Rh crucible in air atmosphere and then made a plate with a metal roll and carbon plate at room temperature (RT).

2.2 Characterization

The elemental analysis of extracted solutions was measured by inductively coupled plasma atomic emission spectroscopy (ICP-AES, Agilent Technologies, USA). To evaluate the molecular structures of the prepared glasses, ^{29}Si, ^{11}B and ^{27}Al magic angle spinning nuclear magnetic resonance (MAS-NMR) spectra were recorded by a Avance III HD 500 MHz spectrometer (Bruker, USA). The resonance frequencies for ^{27}Al, ^{11}B and ^{29}Si are 160.5 MHz, 130.4 MHz and 99.3 MHz, respectively. ^{27}Al MAS-NMR spectra were recorded at a rotation frequency of 12.0 kHz, using a pulse length of 0.60 μs (10° liquid pulse length) and relaxation time of 0.5 s. Chemical shifts were referenced to aqueous solutions of 1 mol/L $Al(NO_3)_3$. ^{11}B MAS-NMR spectra were obtained at a spinning speed of 10 kHz. The pulse length was set as 0.83 μs (15° liquid angle) with a recycle delay of 8 s. Chemical shifts were referenced to 1 mol/L H_3BO_3 solution. ^{29}Si MAS-NMR spectra were acquired at a spinning speed of 6 kHz. Typical pulse length was 2 μs (30° solid flip angle) with a recycle delay of 350 s. Chemical shifts were referenced to Tetrakis (trimethylsilyl) silane.

The microstructures of the prepared samples were studied by energy dispersive X-ray (EDX) mapping and scanning electron microscopy (SEM) using a ULTRA-55 system (Hitachi, Japan). The SEM samples were coated with Pt before performing the measurement. X-ray photoelectron spectroscopy (XPS) measurements were performed with a Escalab250Xi spectrometer (Thermo Scientific, UK), using a monochromatic Al K_α radiation source. All spectra were calibrated using inorganic carbon peak (284.80 eV) as a reference. The density of the as-melt glasses was measured using the Archimedes method. The optical images were recorded using a BX53M optical microscope equipped with a SC180-CCD camera (OLYMPUS, Japan). All the measurements were carried out at room temperature except for those specially stressed.

The hydrolytic resistance test was carried out based on the latest versions of the United States Pharmacopoeia <660>(USP<660>) and European Pharmacopoeia (3.2.1) (EP (3.2.1)) glass grains tests for pharmaceutical glass containers. In these tests, the as-melt glasses ($70SiO_2$-$(20–x)B_2O_3$-xAl_2O_3-$10Na_2O$, x=0, 5%, 10%, 15% and 20%) were crushed using aluminum oxide mortar and pestle inside a fume hood to pulverize the as-melt glasses into grains with sizes of 300–425 μm using coarsest sieves. The glass grains (GGs) were transferred into 100 mL beakers and rinsed by acetone for three times in an ultrasonic bath

for 1 min till the supernatant liquid becomes clear. The beakers were covered by pierced aluminum foils and dried at 120 ℃ for 20 min, which were then transferred from hot air oven to desiccators to cool down the GGs slowly to room temperature.10 g of dried GGs and 50 mL of deionized water (DW) were transferred to a 250 mL quartz conical flask and covered well with a quartz cap. Another 250 mL quartz conical flask containing 50 mL of DW was used as a reference. These two flasks were placed into an autoclave for heat treatment at 121 ℃ for 30 min. The temperature profile of autoclaving was as follows: (1) ramping from RT to 105 ℃; (2) dwelling at 105 ℃ for 10 min; (3) ramping from 105 ℃ to 121 ℃ at heating rate of 1 ℃/min; (4) keeping at 121 ℃ for 30 min; (5) cooling down from 121 ℃ to 105 ℃ at cooling rate 0.5 ℃/min; (6) cooling down from 105 ℃ to 95 ℃ naturally. In order to clearly investigate the structural differences of the GGs before and after autoclaving, the similar temperature profile was used but the autoclaving temperature was changed to 135 ℃ for 16 h (*i.e.* step 4). When the autoclaves were cooled to 95 ℃, the flasks were transferred to a tray filled with hot DW for cooling to RT within 30 min in air. After cooling to RT, the inner surface of these conical flasks and their caps were rinsed with 15 mL DW and then the extracted solutions without GGs were transferred to 250 mL beakers. This step was repeated twice (total three times). Methyl red was used as a pH value indicator by adding 50 μL of methyl red solution to the extracted solutions which turned their color to red and yellow for reference and grains extracted solutions, respectively. This color change indicates that the glass extracted solutions are base solutions as a result of the dissolution of a part of constituent elements of glass during autoclaving. Finally, the extracted solutions were titrated with diluted hydrochloric acid (HCl) (0.02 mol/L) until the yellow color became red and matched the color of reference solution, such that the consumption of HCl divided by the mass of glass grains (*i.e.* 10 g) could be determined.

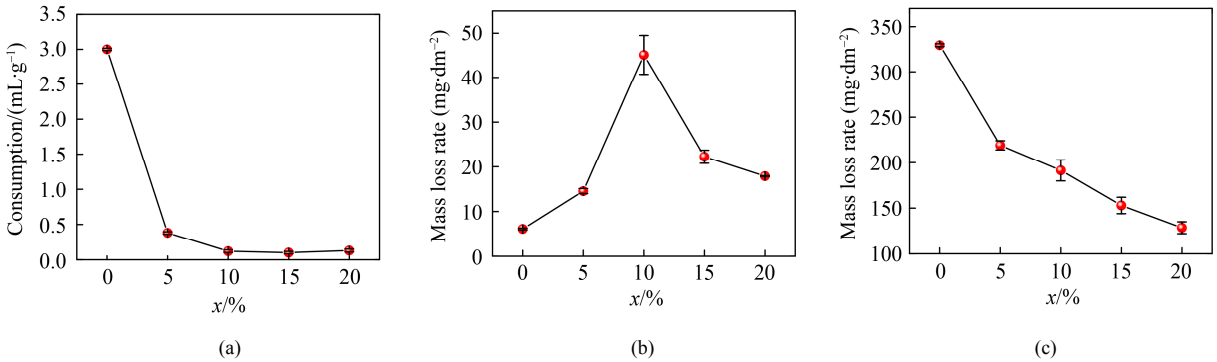
The acid and alkali resistance tests were performed based on an international standards of the Deutsches Institut Fur Normung 12116 (DIN 12116) test and International Organization for Standardization 695 (ISO 695) test, respectively. In these standards, the polished glass plates with dimensions of 25 mm× 30 mm×3 mm (surface area is approximately 15 cm^2) were etched in an aqueous acid solution (22 mol/L of HF+2 mol/L of HCl) at RT for 10 min under stirring. After etching, the glass plates were rinsed for several times by DW and ethanol using an ultrasonic cleaner and then dried at 110 ℃ for 1 h. After drying, the glass samples were cooled to RT in the desiccators within 30 min and finally we measured the sample mass. Polytetrafluoroethylene (PTFE) containers (120 mL) were filled with 6 mol/L of HCl or a mixture of 1 mol/L of NaOH+0.5 mol/L of Na_2CO_3 aqueous solutions. These containers were capped and then heated to 100 ℃ and dwelled for 1 h. Afterwards, the glass plates were placed into the hot aqueous HCl or NaOH solutions at 100 ℃ for 6 h or 3 h, respectively. After the solutions were cooled to RT, the extracted solutions were analyzed by inductively coupled plasma atomic emission spectroscopy for concentrations of elements, such as (Si, Al, B and Na) and (Si, Al and B) for HCl or NaOH solutions, respectively. In addition, the heat-treated glass plates were rinsed for several times by DW and ethanol using ultrasonic path and then dried at 110 ℃ for 1 h. After cooling the glass samples to RT in the desiccators within 30 min, we measured the sample mass and then calculated the mass loss per surface area in mg/dm^2.

3 Results and discussion

3.1 Liquid resistance test and the elemental analysis of the extracted solutions

The chemical durability of the as-melt glasses $70SiO_2$-$(20–x)B_2O_3$-xAl_2O_3-$10Na_2O$ (in mole fraction), x=0, 5, 10, 15 and 20 was first examined by hydrolytic resistance test at 121 ℃ for 30 min (see Fig. 1(a)). It can be observed that the HCl consumption as x=0 has a maximum value at 3 mL/g, indicating the poor chemical stability of this glass against water as result of dissolution of a large amount of constituent elements of glass during autoclaving. However, the introduction of Al_2O_3 significantly enhances the chemical durability of glass and the HCl consumption is reduced to 0.1 mL/g as x=15 and to 0.13 mL/g as x=20[22].

The stability of these glasses against HCl and NaOH aqueous solutions was also investigated by acid or alkali resistance tests. The results are shown in Fig. 1(b) and Fig. 1(c). In Fig. 1(b), after heat treating the as-melt glasses into HCl aqueous solution, the mass loss of glass displays 45.1 mg/dm^2 as x=10, which slowly decreases to 6.1 mg/dm^2 and 17.9 mg/dm^2 as x-value moves to 0 and 20, respectively. In Fig. 1(c), nevertheless, the mass loss per surface area of glass after heat treatment in NaOH aqueous solution at 100 ℃ for 3 h demonstrates a gradual decrease from 329.5 mg/dm^2 to 128.5 mg/dm^2 as x-value increases from 0 to 20. In general, these results imply that the addition of Al_2O_3 into borosilicate glass network improves the glass resistance towards attack in water and NaOH aqueous solutions through reducing the mobility of alkali ions[17–19,23].



(a) HCl consumption per gram at different values of x mole fraction after autoclaving in water at 121 ℃ for 30 min using standards of USP <660> and EP (3.2.1). Glass mass loss as a function of x-value after heat treatment in (b) HCl (using DIN 12116 standard) and (c) NaOH (using ISO 695 standard) aqueous solutions at 100 ℃ for 6 h and 3 h, respectively.

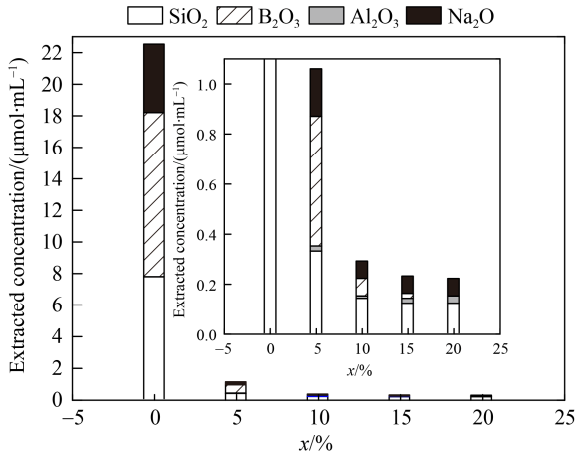
Fig. 1 Dependence of mass loss on Al_2O_3 concentration in the corrosion tests

After heat treatment of the as-melt glasses in water (121 ℃ for 30 min), NaOH (100 ℃ for 3 h) or HCl (100 ℃ for 6 h) aqueous solutions, the compositions of extracted solutions were analyzed using ICP-AES in order to determine the dissolved glass elements and its concentration in the solutions. Fig. 2 shows the concentrations of dissolved glass constituents, confirming the dissolution of all constituents of glass (*e.g.*, SiO_2, B_2O_3, Al_2O_3 and Na_2O) in water, HCl and NaOH aqueous solutions during heat treatment. In Fig. 2(a), the total concentration of dissolved glass as x=0 in water is 22.53 μmol/mL, which contains SiO_2, B_2O_3 and Na_2O. This concentration reduces drastically to 1.04 μmol/mL, 0.29 μmol/mL, 0.23 μmol/mL and 0.19 μmol/mL as x=5, 10, 15 and 20, respectively. In Fig. 2(b), the total dissolved glass concentration in HCl aqueous solution is 0.94 μmol/mL as x=0, which increases to 2.9 μmol/mL and then decreases to 1.77 μmol/mL as x=10 and 20, respectively. In Fig. 2(c), the total extracted concentration in NaOH aqueous solution decreases from 17.03 μmol/mL to 6.1 μmol/mL with increasing x-value from 0 to 20. These results are in reasonable agreement with the discussed results of glass mass loss and HCl consumption (see Fig. 1). According to the analysis of the total extracted concentration of glasses after autoclaving, we could conclude that the chemical durability of the as-melt glasses is related to the pH value of aqueous solution[7,24]. The borosilicate glass (*i.e.* x=0) possesses a relatively poor chemical stability against water and NaOH aqueous solutions, however, its resistance is enhanced in HCl aqueous solutions. By steadily replacing B_2O_3 by Al_2O_3, we can find that the chemical robustness of glass network is considerably improved in water and NaOH aqueous solution, while the as-melt glasses demonstrate a decrease in their chemical durability after heat treatment in HCl aqueous solution.

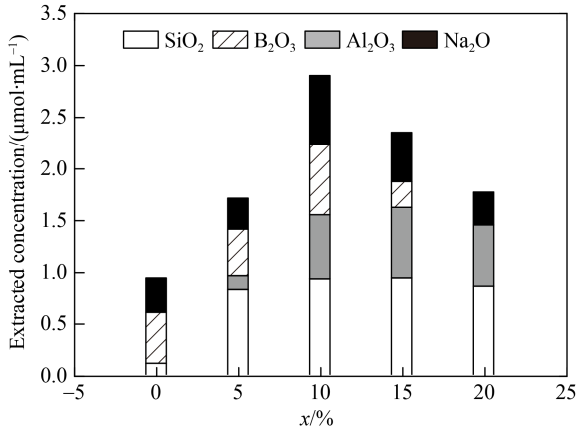
To compare the composition difference between the as-melt glasses and the dissolved glasses during autoclaving, the extracted concentration (in mole fraction) were calculated based on the results in Fig. 2. Fig. 3 shows the calculated results. It is interesting to note that the extracted concentrations (in molar fraction) of all dissolved glasses in different solutions show an increase in Al_2O_3 and deficiency in B_2O_3 with increasing x-value, which is similar to the change in the as-melt glass composition (see Fig. 3(a)). The pH value of the solution and the glass composition strongly affects the selective erosion of glass constituents through ion exchange between (Si, Al, B and Na) and (H and OH)[7]. For instance, as x=0 (see Fig. 3(c)), acidic aqueous solution prefers to erode Na_2O (36.17%) and B_2O_3 (52.13%) rather than SiO_2 (11.7%), while the erosion preference is changed with the addition of Al_2O_3 into the glass network. Consequently, the extracted concentration of Na_2O steadily decreases to 18.08% as x=20; however, the concentration of SiO_2 (48.59%, x=20) increases with increasing x-value.

In addition, the concentration of Al_2O_3 increases to 33.33% as x=20. This result indicates that HCl aqueous solution prefers to corrode Na_2O and Al_2O_3 instead of SiO_2 as x=20. The unexpected values of concentration ratios as x=5 indicate that the glass network is not uniform near the surface. Similar to HCl aqueous solution, the dissolved glass components into water as x=0 (see Fig. 3(b)) contains SiO_2, B_2O_3 and Na_2O with concentrations of 34.31%, 46.38% and 19.31%, respectively. The extracted concentrations of SiO_2, Al_2O_3 and Na_2O at x=20 significantly change to 54.54%, 13.64% and 31.82%, respectively, with the increase of Al_2O_3 content in the glass. These results indicate that B_2O_3 and Na_2O are etched out more quickly as x=0. Furthermore, the dissolved glass components into NaOH aqueous solution (see Fig. 3(d)) at different x-values demonstrates a high concentration

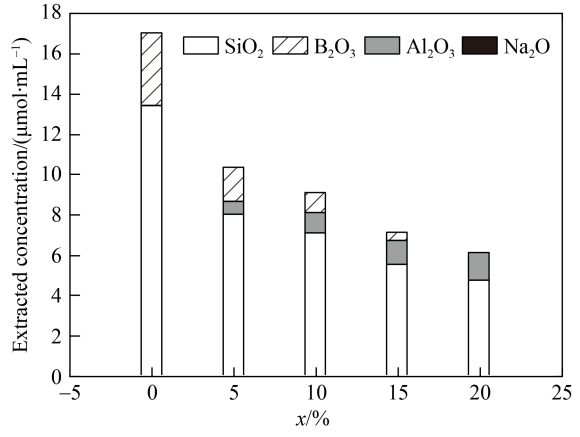
of SiO_2 for all glasses, which is almost unchanged at 78%, while the concentrations of B_2O_3 and Al_2O_3 are comparable to the glass composition variation. This observation means that SiO_2 component suffers a faster dissolution in solutions with greater pH values. We could not measure Na_2O concentration because of using NaOH aqueous solution.



(a) Water at 121 ℃ for 30 min



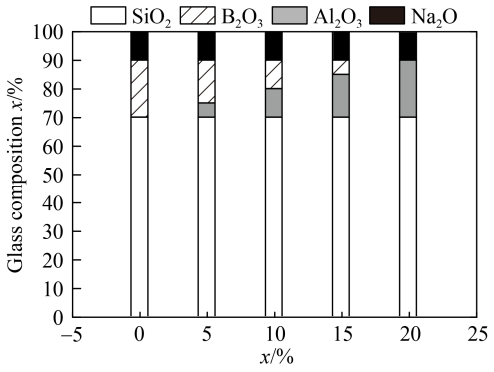
(b) HCl solution at 100 ℃ for 6 h



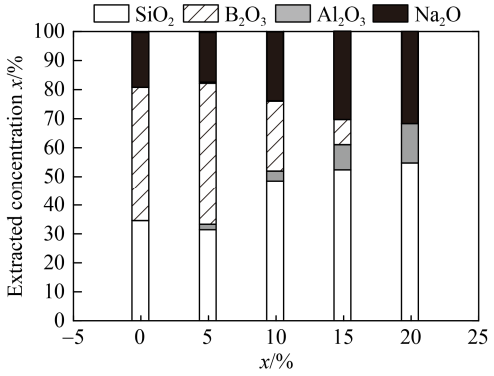
(c) NaOH solution at 100 ℃ for 3 h

The inset of (a) shows the magnified statistics at low concentration values.

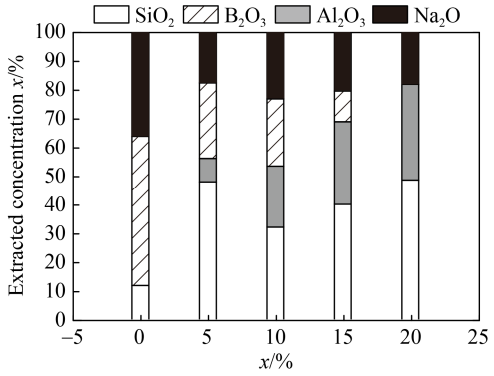
Fig. 2　Extracted concentration of the heat treated glass grains at different *x*-values



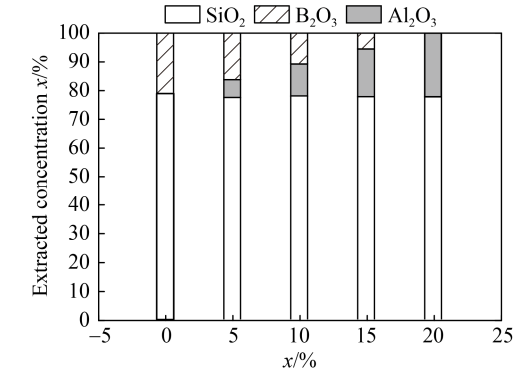
(a) Nominal composition



(b) Water at 121 ℃ for 30 min



(c) HCl solution at 100 ℃ for 6 h

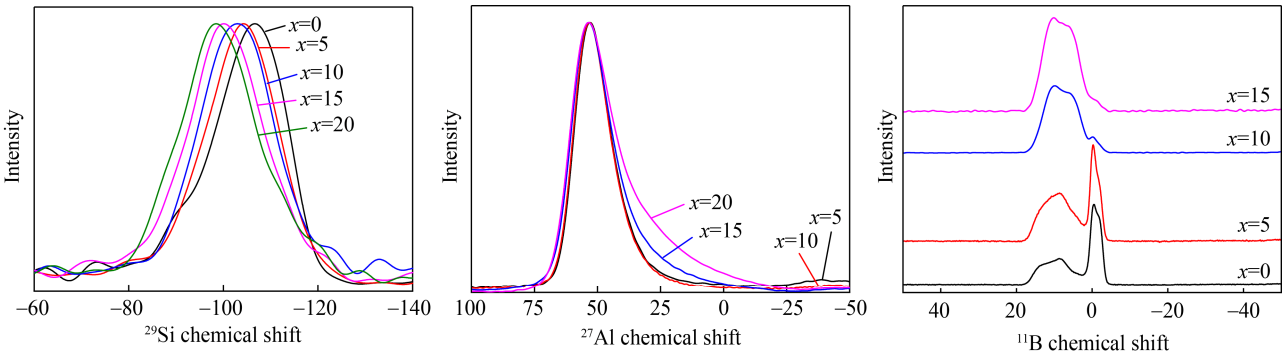


(d) NaOH solution at 100 ℃ for 3 h

Fig. 3　Composition analysis of the glass before and after different treatments

3.2 Local structure characterizations of the as-melt glasses

Fig. 4 shows the ^{29}Si, ^{27}Al and ^{11}B MAS-NMR spectra for the as-melt glasses $70SiO_2$-$(20–x)B_2O_3$-xAl_2O_3-$10Na_2O$ as x=0, 5, 10, 15 and 20, respectively. In Fig. 4(a), the ^{29}Si MAS-NMR spectra demonstrate that the tetrahedral SiO_4 structures with four-bridging oxygen (BO) (Q^4, *i.e.* SiO_4(0B,4Si)) are dominant (–106.5) in the as-melt glass as x=0, while, a few number of the tetrahedral SiO_4 species with one-bridging BO (Q^1, *i.e.* SiO_4(3B, 1Si)) (–89.2) also exist in the glass network[25–26]. Also, the gradual addition of Al_2O_3 into the glass network leads to the complete turning of Q^4 into Q^3 (–98.5) (*i.e.* SiO_4(1Al, 3Si)) as x=20 in addition to the disappearing of Q^1. The structure differences at a molecular level were deeply investigated by ^{27}Al and ^{11}B MAS-NMR spectra (see Fig. 4(b)) and Fig. 4(c)). In Fig. 4(b), a sharp peak at 53.3 was recorded for all of the as-melt glasses, which can be attributed to the presence of four-fold coordinated aluminum ions Al(IV) among glass matrices[27]. Furthermore, the bulge at 25 of the samples as x=15 and 20 refers to the existence of five-fold coordinated aluminum ions Al(V) with a low concentration. In Fig. 4(c), the ^{11}B MAS-NMR spectra reveal that the as-melt glass as x=0 contains triangle BO_3 (13 and 8) as well as tetrahedral BO_4 (–0.5 and –2.0) units. As x-value increases, the number of BO_3 units increases rather than BO_4 units, implying that the gradual addition of Al_2O_3 into glass network induces boron to coordinate with oxygen in triangle shape instead of pyramidal structure[28–29].



(a) ^{29}Si (b) ^{27}Al (c) ^{11}B MAS-NMR

Fig. 4 Solid-state NMR spectra of the as-melt glasses$70SiO_2$-$(20–x)B_2O_3$-xAl_2O_3-$10Na_2O$

In Fig. 5, we observed that BO_3 can exist in the forms of ring (13) and non-ring (8) structures, however, BO_4 sites are surrounded by four Si atoms with four-non-bridging oxygen (NBO) (*i.e.* BO_4(0B, 4Si), –2) or connected with one B atom and three Si atoms with three NBO (*i.e.* BO_4(1B,3Si), –0.5).[29] Fig. 6 shows the calculated relative fraction of $BO_{3\ ring}$, $BO_{3\ nonring}$, BO_4 (1B, 3Si) and BO_4 (0B, 4Si) units in the as-melt glasses (x=0, 5, 10 and 15). The relative fraction of the BO_3 and BO_4 structures strongly relies on x-value, where, the BO_4 units (*i.e.* BO_4(1B, 3Si) and BO_4(0B, 4Si)) are gradually converted to BO_3 units (*i.e.* $BO_{3\ ring}$ and $BO_{3\ nonring}$) as x-value increases from 0 to 15. The total relative fractions of BO_3 (*i.e.* $BO_{3\ ring}$+$BO_{3\ nonring}$) and BO_4 (*i.e.* BO_4 (1B,3Si)+BO_4 (0B,4Si)) are 51.79% and 48.21% at x=0, respectively. As x=15, the relative fractions of BO_3 and BO_4 are 99.47% and 0.53%, respectively.

From the NMR results, we could explain the enhancement of chemical durability of glasses with increasing the content of Al_2O_3 in the glass network. For instance, the extracted concentration of boron as x=0 (see Fig. 2(a), water treatment) is 10.45 μmol/mL in which the relative fractions of BO_3 and BO_4 (see Fig. 6) are 51.79% and 48.21%, respectively. However, as x=10, the extracted concentration of boron decreases to 0.52 μmol/mL and the relative fractions of BO_3 and BO_4 are 99% and 1%, respectively. This means that BO_4 units are highly soluble into water in comparison to BO_3 units. Accordingly, we conclude that the poor chemical durability of Al_2O_3 free borosilicate glass is correlated to the existence of BO_4 with three and four NBO in the glass matrix. Moreover, the substitution of BO_4 by AlO_4 plays a significant role in improving the chemical durability of borosilicate glass through replacing the NBO of BO_4 (*i.e.*, Si−O−B) by the BO of AlO_4 (*i.e.*, Si−O−Al) and the conversion of BO_4 into BO_3. These changes result in toughening of the glass network and make the glasses more robust against water and NaOH aqueous solution[24].

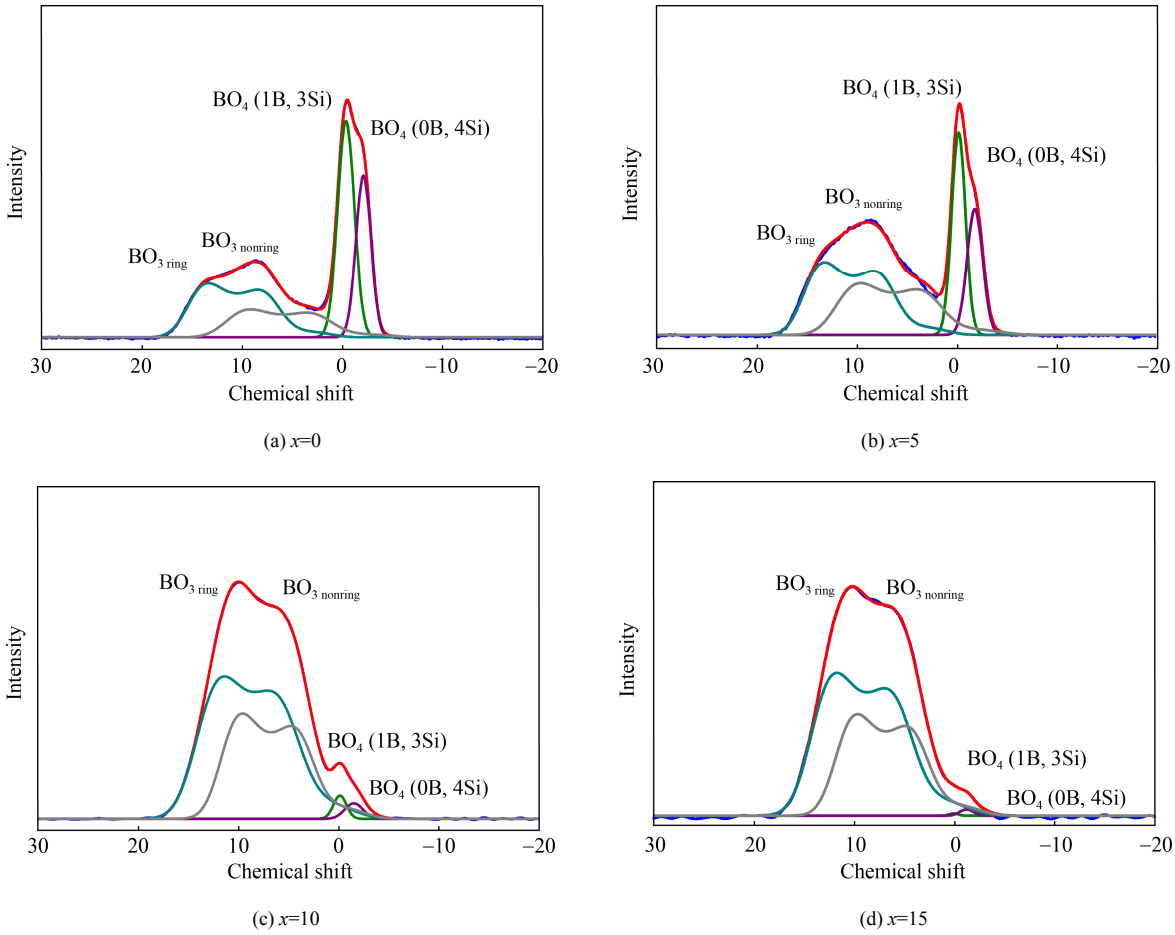


Fig. 5　Deconvolution of the ^{11}B MAS-NMR spectra of the as-melt glasses $70SiO_2$-$(20–x)B_2O_3$-xAl_2O_3-$10Na_2O$

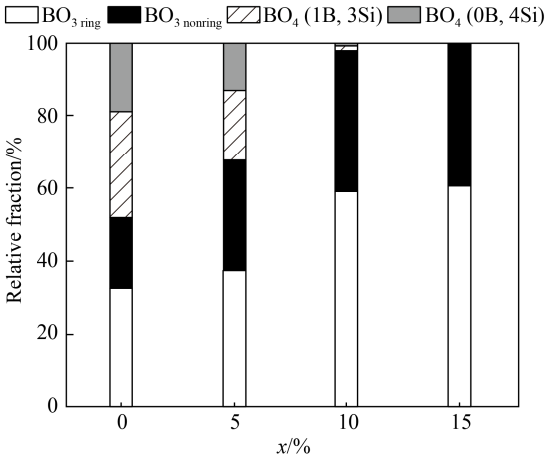


Fig. 6　Relative fractions of B species ($BO_{3\ ring}$, $BO_{3\ nonring}$, BO_4 (1B, 3Si) and BO_4 (0B, 4Si)) in the as-melt glasses $70SiO_2$–$(20–x)B_2O_3$–xAl_2O_3–$10Na_2O$ @ x=0, 5, 10 and 15

Fig. 7 shows the density and molar volume of glasses in HCl aqueous solution. Clearly, the glass density decreases from 2.36 g/cm^3 to 2.30 g/cm^3 as the x-value increases from 0 to 10. This value (*i.e.*, x=10) grows to 2.36 g/cm^3 and 2.42 g/cm^3 as x=15 and 20, respectively. In contrast to the values of glass densities, the molar volume of glass as x=0 is 26.37 cm^3/mol, which significantly increases to 28.43 cm^3/mol as x-value increases to 10. In addition, the molar volume slightly decreases to 28.42 cm^3/mol and 28.41 cm^3/mol as x=15 and x=20, respectively. This result implies that the molecular space of network is enlarged as x=10, which allows the soaking of HCl aqueous solution efficiently that leads to the corrosion of glass more severely, while the network molecular space shrinks

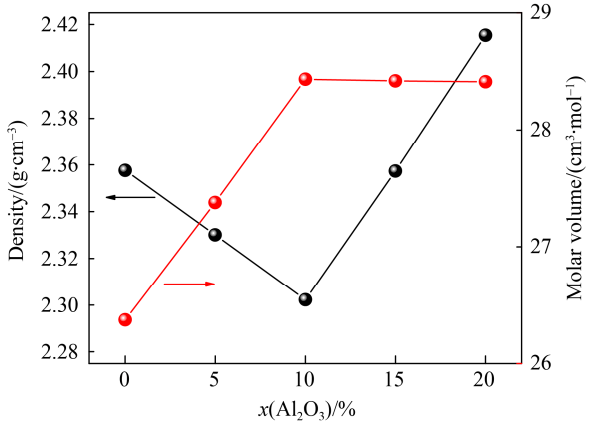
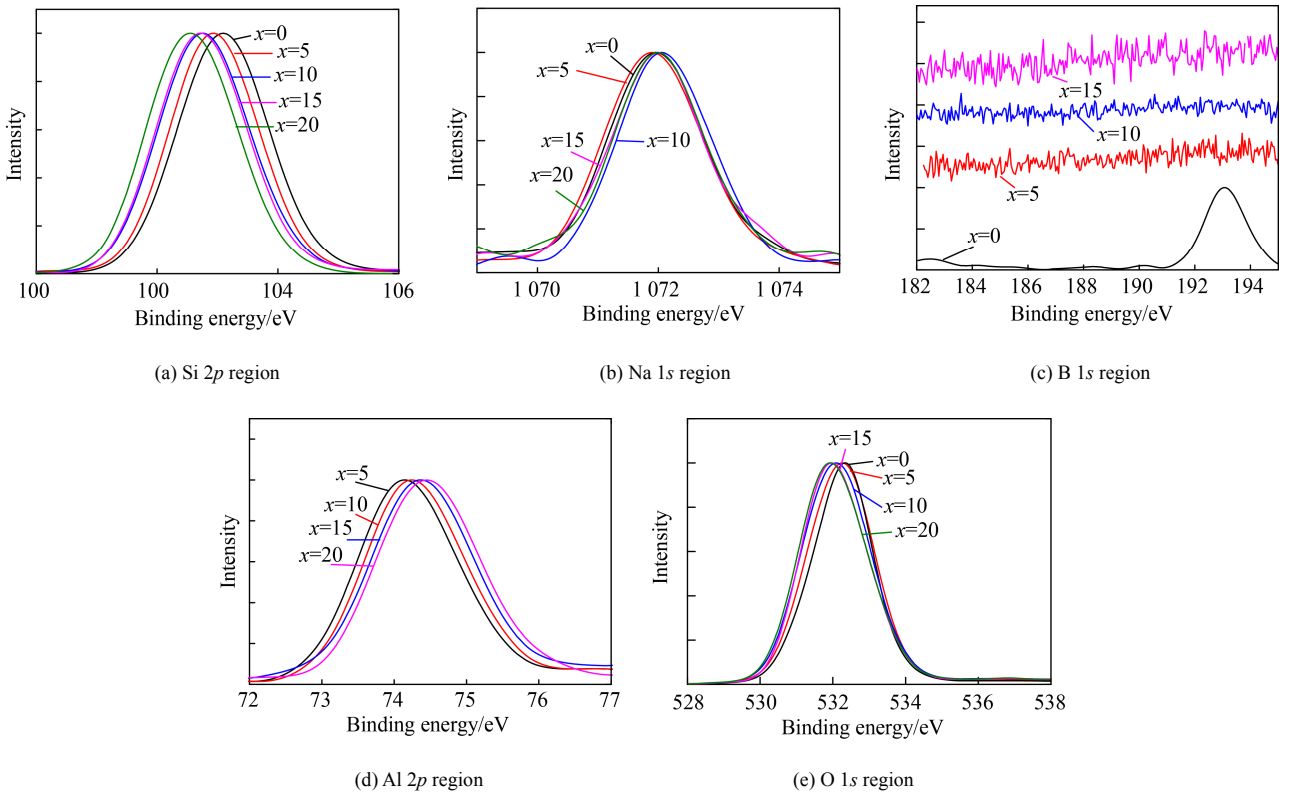


Fig. 7　Density and molar volume of the $70SiO_2$–$(20–x)B_2O_3$–xAl_2O_3–$10Na_2O$ bulk glasses @ x=0, 5, 10, 15 and 20

notably as x=0, blocking the diffusion of chlorine ions with a large ionic radius (1.81 pm)[7,17,22–23]. These results may explain the observed mass loss peak as x=10 for the corrosion experiment performed in HCl aqueous solution.

Fig. 8 shows the XPS spectra of the as-melt bulk glasses. The results show that the as-melt glasses as x=0 have typical peaks of Si 2p (Si−O), Na 1s (Na−O), B 1s (B−O) and Al 2p (Al−O) regions with obvious bonding to oxygen at 103.1 eV (see Fig. 8(a)), 1 072 eV (see Fig. 8(b)), 193.1 eV (see Fig. 8(c)), 74.15 eV (see Fig. 8(d)), respectively[26–29]. The addition of Al_2O_3 into glass network significantly changes Si 2p peak position, which gradually shifts to 102.55 eV as x=20 as result of the conversion of Q^4 into Q^3 (see Fig. 8(a))[30–31]. Similar to the Si 2p-XPS spectra, the Al 2p-XPS spectra of the as-melt glasses (see Fig. 8(d)) turn from 74.15 eV into 74.45 eV with increasing x-value from 0 to 20 due to the formation of Al(V)[32–33]. The Na 1s-XPS spectra of the as-melt glasses at different x-values (see Fig. 8(b)) do not exhibit an apparent change in the peak position, indicating that the chemical environment of Na does not change. In addition, we could not observe B 1s signal as x=5, 10 and 15 (see Fig. 8(c)) because of the low content of B on glass surface. The O 1s-XPS of the as-melt glass as x=0 (see Fig. 8(e)) demonstrates a peak at 532.25 eV, which is attributed to the BO of Si−O−Si. This peak steadily moves to 531.95 eV as x=20, confirming the conversion of SiO_4 from Q^4 to Q^3. The XPS results of the as-melt bulk glasses are in reasonable agreement with the NMR results and confirm the conversion of Q^4 into Q^3 with increase of x-value as well as the formation of Al(V) in the glass at a great content of Al_2O_3.



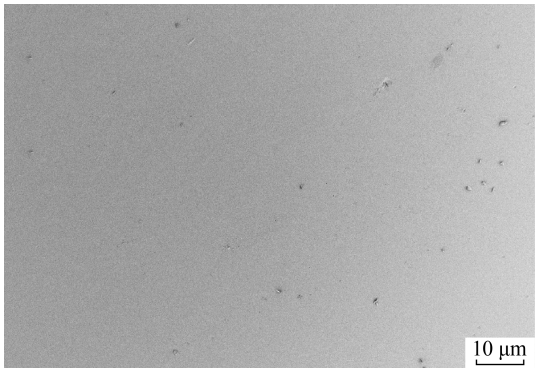
(a) Si 2p region (b) Na 1s region (c) B 1s region

(d) Al 2p region (e) O 1s region

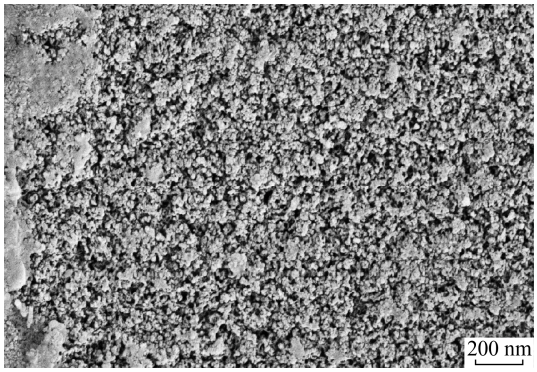
Fig. 8 XPS spectra of the as-melt bulk glasses at different x-values

3.3 Structural difference of the glass surface before and after autoclaving:

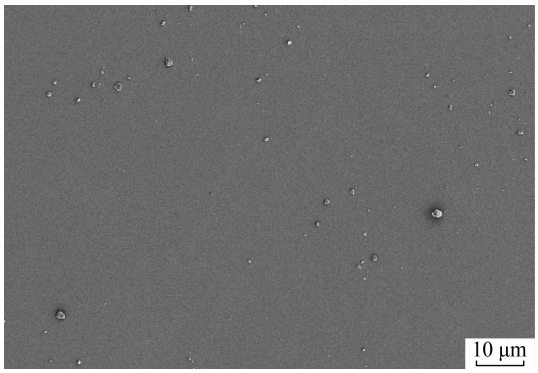
Fig. 9 shows the SEM images of treated bulk glasses in water (x=0, 20) at 135 ℃ for 16 h. As x=20 (see Fig. 9(c) and Fig. 9(d)), there is no observable change in the morphology of glass surface before and after autoclaving. This is because of the relatively low HCl consumption (0.13 mL/g), indicating that low amounts of Si, Al and Na ions are dissolved into water during heat treatment (see Fig. 2(a) and Fig. 3(a)). In comparison, as x=0 (see Fig. 9(a) and Fig. 9(b)), the surface microstructure of treated glass differs greatly from that of untreated glass. In contrast to the observed smooth surface of the as-melt glasses, a porous structure appears on the surface of the heat-treated glass, which can be related to the dissolution of Si, B and Na in hot water during the autoclaving process[15,20]. The similar results are observed using optical microscopy for glasses as x=0, 20 before and after heat treatment (see Fig. 10).



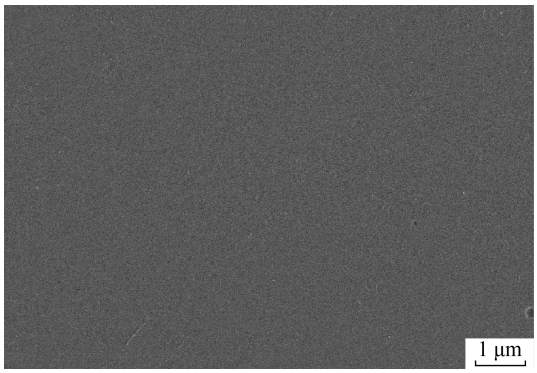
(a) Before autoclaving



(b) After autoclaving in water at 135 ℃ for 16 h



(c) Before autoclaving

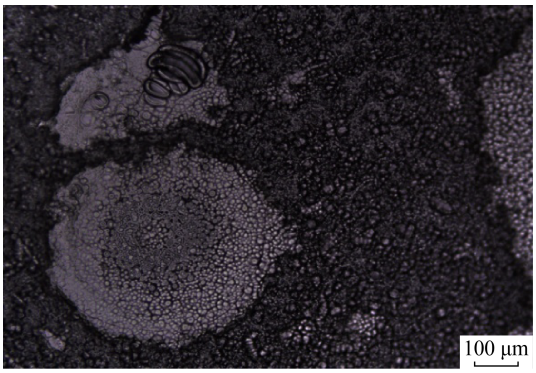


(d) After autoclaving in water at 135 ℃ for 16 h

Fig. 9 SEM images of the (a,b) $70SiO_2$–$20B_2O_3$–$10Na_2O$ and the (c,d) $70SiO_2$–$20Al_2O_3$–$10Na_2O$ bulk glasses



(a) Before autoclaving



(b) After autoclaving in water at 135 ℃ for 16 h



(c) Before autoclaving



(d) After autoclaving in water at 135 ℃ for 16 h

Fig. 10　Optical images of the (a,b) $70SiO_2$–$20B_2O_3$–$10Na_2O$ and the (c,d) $70SiO_2$–$20Al_2O_3$–$10Na_2O$ bulk glasses

To further examine the porous structure on the surface of the heat-treated bulk glass as x=0, EDX mappings and SEM observation were carried out. The results are shown in Fig. 11 and Fig. 12. Clearly, the distributions of Si, O and Na atoms are homogeneous, confirming the dissolution of constituent elements of glass during autoclaving.

In order to evaluate the atomic structure differences of glass surface before and after autoclaving process, the XPS spectra were measured for the heat-treated bulk glasses (x=0, 10 and 20) in water (see Fig. 13–Fig. 14), HCl (see Fig. 15 and Fig. 16), and NaOH (see Fig. 17–Fig. 18) aqueous solutions. After heating the bulk glasses (x=0, 10, and 20) in water and NaOH aqueous solution, we see that Si 2p, Na 1s, B 1s and Al 2p XPS spectra of the heat-treated glasses are identical to that of the untreated glasses. As x=0, the O 1s spectra

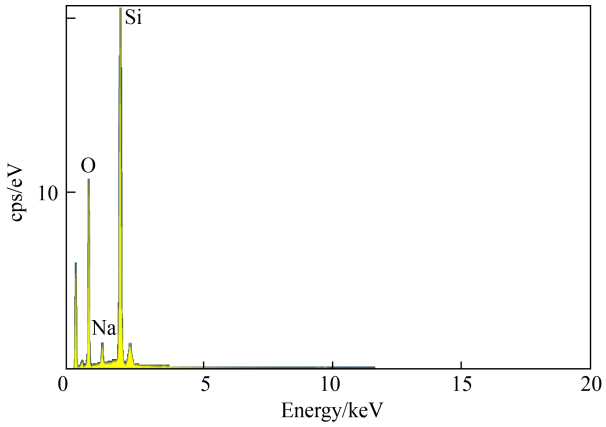
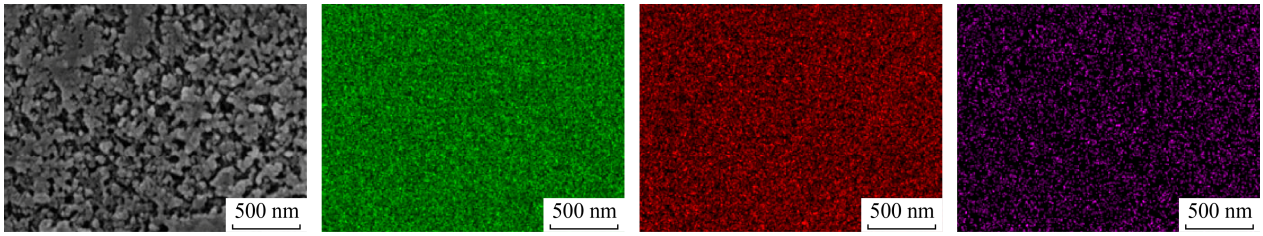


Fig. 11 EDX spectra of the $70SiO_2$–$20B_2O_3$–$10Na_2O$ bulk glass after autoclaving process in water at 135 ℃ for 16 h



(a) (b) (c) (d)

B mappings for this glass were not determined due to the EDX instrument limitation.

Fig. 12 (a) SEM images of the $70SiO_2$–$20B_2O_3$–$10Na_2O$ bulk glass after autoclaving process in water at 135 ℃ for 16 h and its EDX mappings for (b) Si, (c) O, and (d) Na

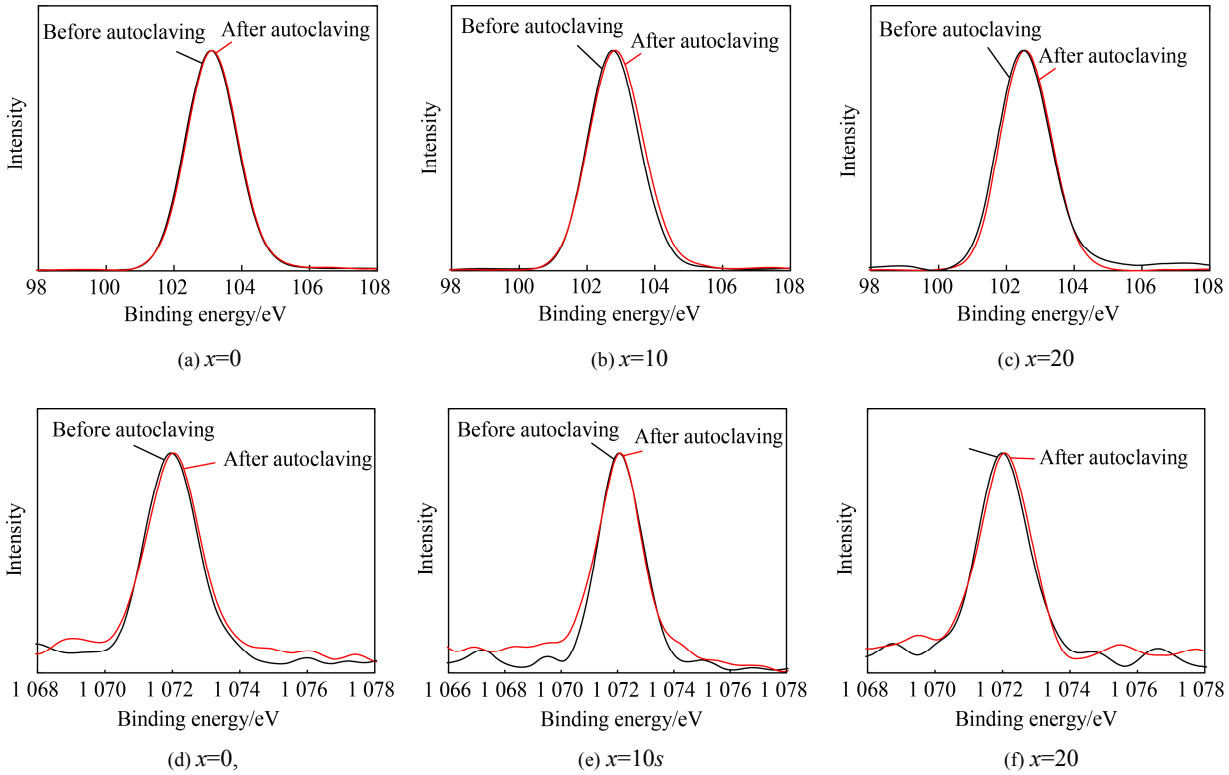
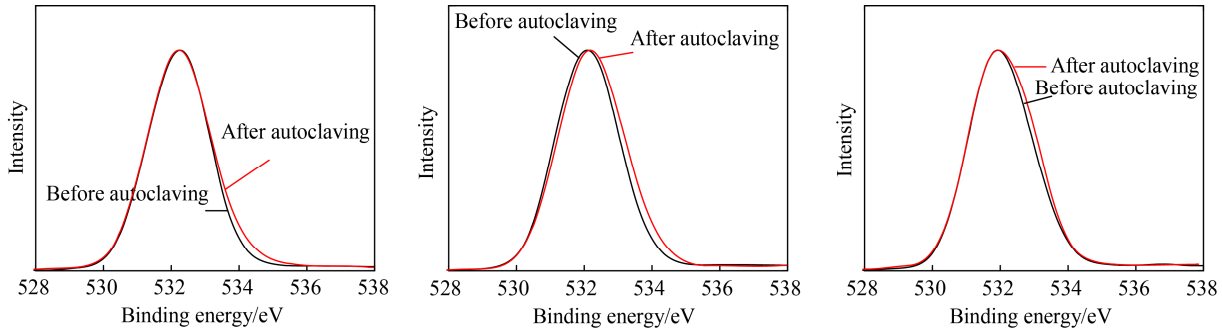
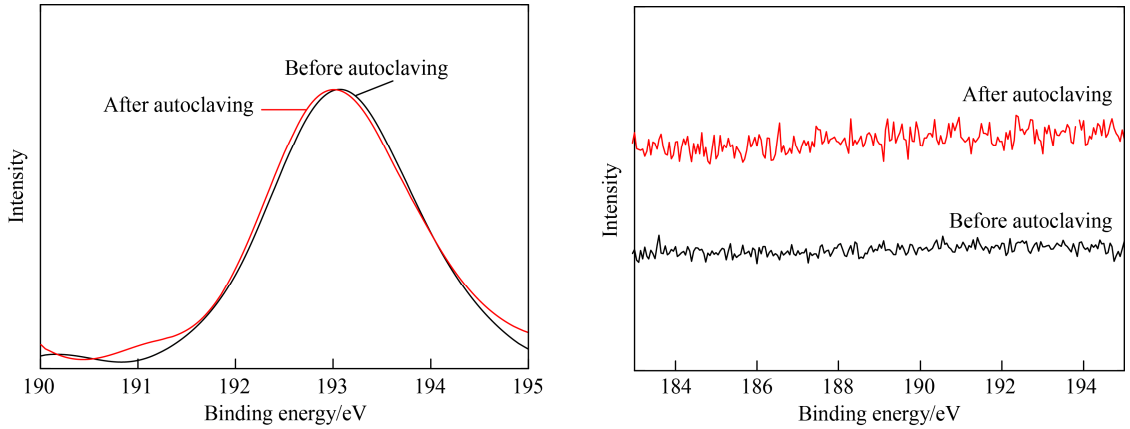


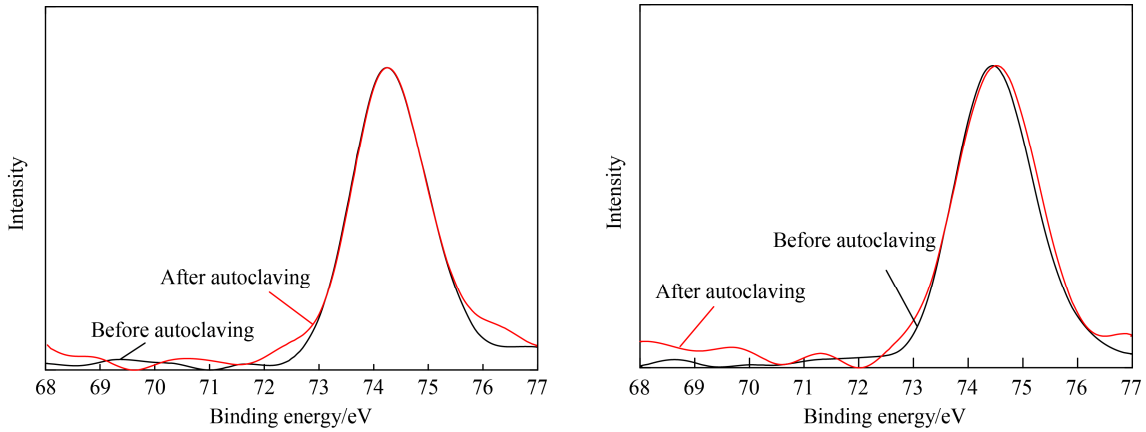
Fig. 13 XPS spectra of the bulk glasses before and after autoclaving in water at 135 ℃ for 16 h



(a) x=0, O 1s　　(b) x=10, O 1s　　(c) x=20, O 1s



(a) x=0, B 1 s　　(b) x=10, B 1 s



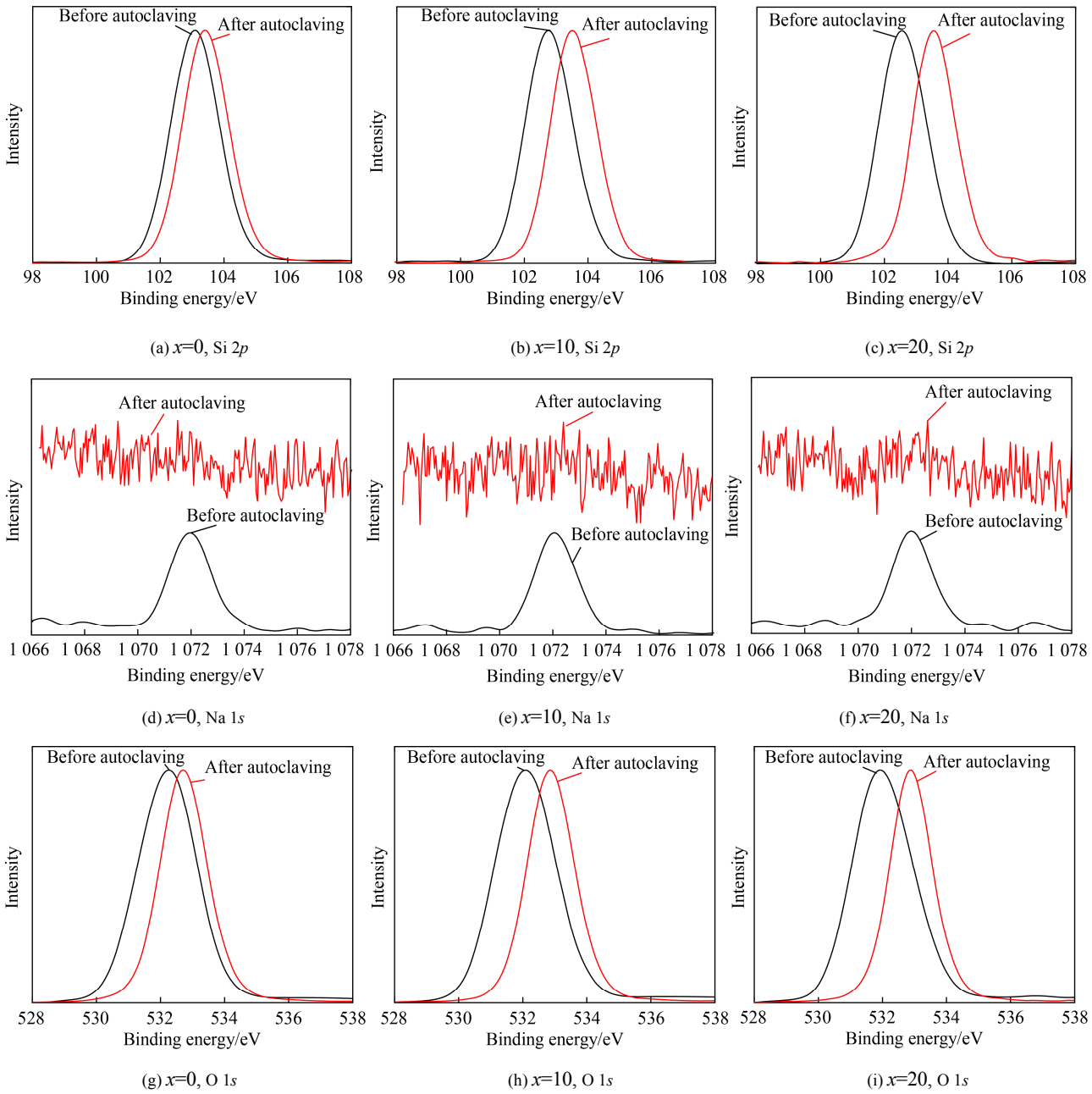
(c) x=10, Al 2p　　(d) x=20, Al 2p

Fig. 14　XPS spectra of the bulk glasses before and after autoclaving in water at 135 ℃ for 16 h

of the heat treated glass in water and NaOH aqueous solution illustrate a bulge at 534 eV, which does not appear in the O 1s spectrum of the untreated glass. The observed bulge is assigned to the existence of Si−O−H group on the glass surface[34–37]. Also, this bulge gradually decreases as x-value reaches to 20. The fading of bulge in the O 1s spectra of the treated glass as x=20 compared with the treated glass as x=0 is due to the dissolution of a small quantity of glass constituent elements into water and NaOH aqueous solution. The XPS results of the treated glasses in water and NaOH aqueous solution are in line with the results of hydrolytic resistance test (see Fig. 1), indicating the dissolution of glass into water and NaOH aqueous solution through ion exchange process. Unlike the heat treatment of glasses in water and

NaOH aqueous solution, the ion exchange effect is strong during autoclaving the as-melt glasses (x=0, 10, and 20) in HCl aqueous solution, where, the Na 1s, B 1s and Al 2p XPS signals disappear after heat treatment as result of the dissolute most of Na, B, and Al located on the glass surface. To clearly observe the process of ion exchange, Si 2p and O 1s XPS spectra were measured for the surface of bulk glasses (x=0, 10 and 20) before and after heat treatment in HCl aqueous solution. It is interesting to note that all Si 2p-XPS peaks shift from 103.1 eV (x=0), 102.75 eV (x=10), and 102.55 eV (x=20) to 103.55 eV, implying the formation of Si−O−H on the glass surface[35–36].

These results indicate that Si−O−(Si/Al/Na/B) chains are dissolved into HCl aqueous solution during autoclaving, forming (Si/Al/Na/B)−O−H in the solution and Si−O−H on the glass surface through an ion exchange process (*i.e.*, (Si−O−(Si/Al/Na/B) + H−O−H => (Si/Al/Na/B)−O−H + Si−O−H). Similar to the Si 2p-XPS spectra, the O 1s-XPS spectra of the heat treated glasses in HCl aqueous solution display a peak shift from 532.25 eV (x=0), 532.1 eV (x=10), and 531.95 eV (x=20) to 532.85 eV as a result of the transformation Si−O−(Si/Al/Na/B) into Si−O−H on the glass surface[36].



(a) x=0, Si 2p (b) x=10, Si 2p (c) x=20, Si 2p

(d) x=0, Na 1s (e) x=10, Na 1s (f) x=20, Na 1s

(g) x=0, O 1s (h) x=10, O 1s (i) x=20, O 1s

Fig. 15 XPS spectra of the bulk glasses before and after autoclaving in HCl aqueous solution at 100 ℃ for 6 h

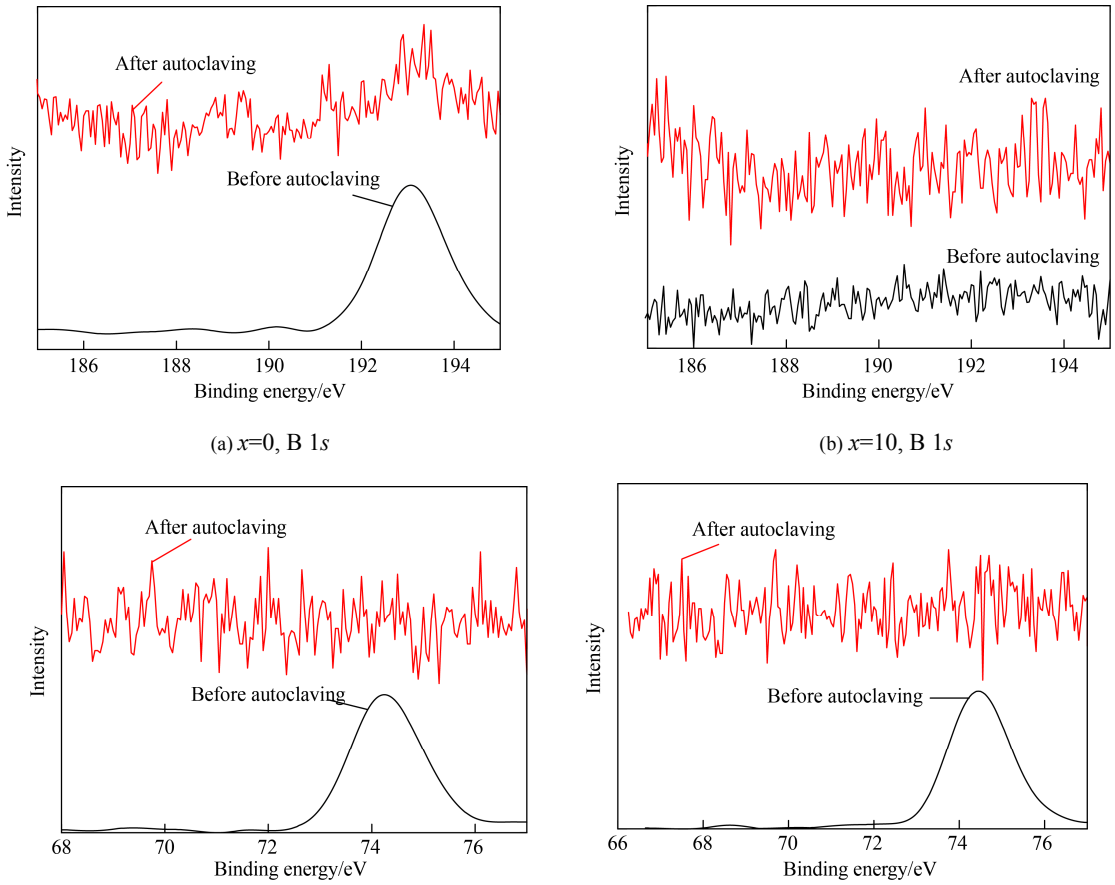


Fig. 16　XPS spectra of the bulk glasses before and after autoclaving in HCl aqueous solution at 100 ℃ for 6 h

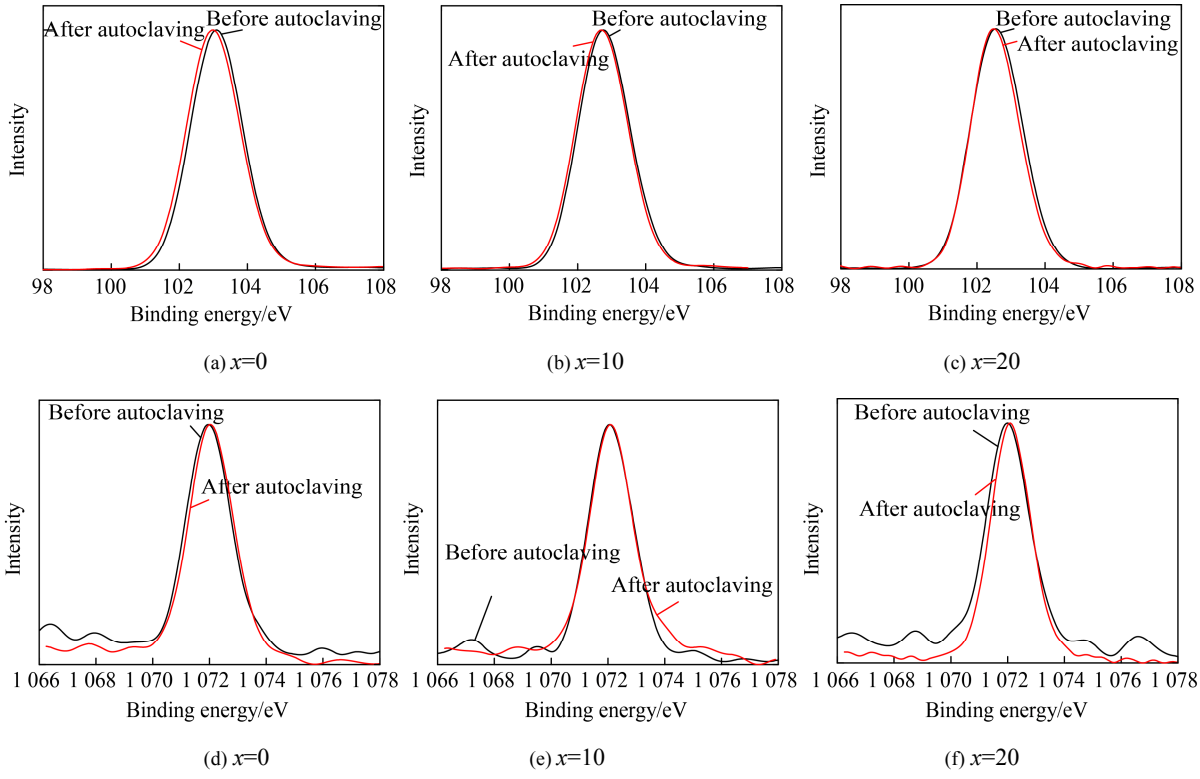
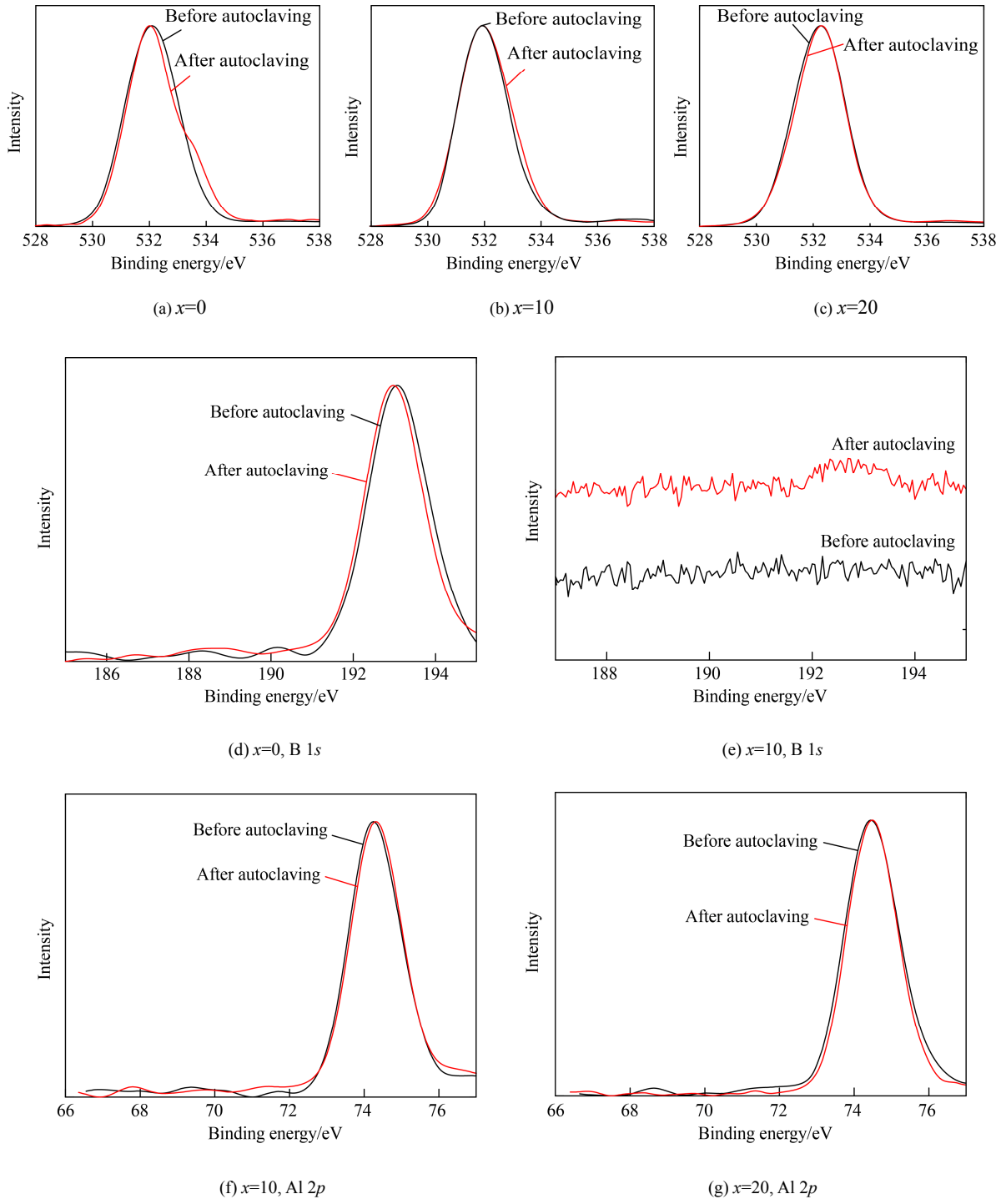


Fig. 17　XPS spectra of the bulk glasses before and after autoclaving in NaOH aqueous solution at 100 ℃ for 3 h



(a) x=0 (b) x=10 (c) x=20

(d) x=0, B 1s (e) x=10, B 1s

(f) x=10, Al 2p (g) x=20, Al 2p

Fig. 18 XPS spectra of the bulk glasses before and after autoclaving in NaOH aqueous solution at 100 ℃ for 3 h

4 Conclusions

The effect of alumina on the chemical durability of borosilicate glasses was examined. The experimental results indicated that the formation of porous glass surface for the Al_2O_3-free glass was associated with the presence of NBO of BO_4 in the as-melt glass. The addition of alumina enhanced the chemical stability of glass to chemical attack in aqueous solutions through reducing the mobility of Na and B ions as well as suppressing the formation of BO_4. We therefore attributed the enhanced chemical robustness of the examined glasses to the replacing of Si−O−B chains by Si−O−Al.

参考文献:

[1] CAILLETEAU C, ANGELI F, DEVREUX F, et al. Insight into silicate-glass corrosion mechanisms[J]. Nat Mater, 2008, 7: 978–983.

[2] GROSS T M, LAHIRI J, GOLAS A, et al. Copper-containing glass ceramic with high antimicrobial efficacy[J]. Nat Commun, 2019, 10: 1979.

[3] HUANG X, GUO Q, YANG D, et al. Reversible 3D laser printing of perovskite quantum dots inside a transparent medium[J]. Nat Photon 2020, 14: 82–88.

[4] LU X, DENG L, KERISIT S, et al. Structural role of ZrO_2 and its impact on properties of boroaluminosilicate nuclear waste glasses[J]. npj Mater Degrad, 2018, 2: 19.

[5] ALI M A, YUEHUI X, LIU X, et al. Self-confined precipitation of ultrasmall plasmonic $Cu_{2-x}Se$ particles in transparent solid medium[J]. J Phys Chem C, 2019, 14: 9394−9399.

[6] ALI M A, REN J, ZHAO T, et al. Broad mid-infrared luminescence in a metal-organic framework glass[J]. ACS Omega, 2019, 4: 12081−12087.

[7] MASCARAQUE N, BAUCHY M, SMEDSKJAER M M. Correlating the network topology of oxide glasses with their chemical durability[J]. J Phys Chem B, 2017, 121: 1139–1147.

[8] SMEDSKJAER M M, MAURO J C, YOUNGMAN R E, et al. Topological principles of borosilicate glass chemistry[J]. J Phys Chem B, 2011, 115: 12930–12946.

[9] KAPOOR S, YOUNGMAN R E, ZAKHARCHUK K, et al. Structural and chemical approach toward understanding the aqueous corrosion of sodium aluminoborate glasses[J]. J Phys Chem B, 2018, 122: 10913−10927.

[10] MASCARAQUE N, BAUCHY M, FIERRO J L G, et al. Dissolution kinetics of hot compressed oxide glasses[J]. J Phys Chem B, 2017, 121: 9063−9072.

[11] PIOVESAN V, BARDEZ-GIBOIRE I, FOURNIER M, et al. Chemical durability of peraluminous glasses for nuclear waste conditioning[J]. npj Mater Degrad, 2018, 2: 7.

[12] XU L, YANG Y,HU ZW, et al. Comparison study on the stability of copper nanowires and their oxidation kinetics in gas and liquid[J]. ACS Nano, 2016, 10: 3823−3834.

[13] OH J H, SHIN H, CHOI J Y, et al. In-plate and on-plate structural control of ultra-stable gold/silver bimetallic nanoplates as redox catalysts, nanobuilding blocks, and single-nanoparticle surface-enhanced Raman scattering probes[J]. ACS Appl Mater Interfaces, 2016, 8: 27140−27150.

[14] HONG S H, CHA M S, HONGSK, et al. Structural effect of the hydrophobic block on the chemical stability of ion-conducting multiblock copolymers for flow battery[J]. ACS Sustainable Chem Eng, 2019, 7: 17088−17099.

[15] MASSERA J, BOURHIS K, PETIT L, et al. Effect of the glass composition on the chemical durability of zinc-phosphate-based glasses in aqueous solutions[J]. J Phys Chem Solids, 2013, 74: 121−127.

[16] LIU X, QIAO Y, QIAN Z, et al. Research on chemical durability of iron phosphate glass waste forms vitrifying SrF_2 and CeF_3[J]. J Nucl Mater, 2018, 508: 286−291.

[17] RAHIMI R A, SADRNEZHAAD S K, RAISALI G. Chemical durability of lead silicate glass in HNO_3, HCl and H_2SO_4 aqueous acid solutions[J]. J Non-Cryst Solids, 2009, 355: 169−174.

[18] FREDERICCI C, YOSHIMURA H N, MOLISANI A L, et al. Effect of TiO_2 addition on the chemical durability of Bi_2O_3–SiO_2–ZnO–B_2O_3 glass system[J]. J Non-Cryst Solids, 2008, 354: 4777−4785.

[19] VARSHNEY A K, MAURO J C. Chapter 17-Chemical durability[M]. Fundamentals of inorganic glasses: 3rd Edition, 2019: 473−486.

[20] SHI Q, YUE Y, QU Y, et al. Structure and chemical durability of calcium iron phosphate glasses doped with La_2O_3 and CeO_2[J]. J Non-Cryst Solids, 2019, 516: 50−55.

[21] ZHAO J, WANG Y, KANG J, et al. Effect of SnO_2 on the structure and chemical durability of the glass prepared by red mud[J]. J Non-Cryst Solids, 2019, 509: 54−59.

[22] ZHU H, WANG F, LIAO Q, et al. Structure features, crystallization kinetics and water resistance of borosilicate glasses doped with CeO_2[J]. J Non-Cryst Solids, 2008, 518: 57–65.

[23] WANG M, CHENG J, LIU Q, et al. The effect of light rare earths on the chemical durability and weathering of Na_2O-CaO-SiO_2 glasses[J]. J Nucl Mater, 2010, 400: 107–111.

[24] CONRADT R. Chemical durability of oxide glasses in aqueous solutions: a review[J]. J Am Ceram Soc, 2008, 91: 728–735.

[25] DHARA H, MISHRA R K, SHUKLA R, et al. A comparative study on the structural aspects of sodium borosilicate glasses and barium borosilicate glasses: Effect of Al_2O_3 addition[J]. J Non-Cryst Solids, 2016, 447: 283−289.

[26] AGUIAR H, SERRA J, GONZALEZ P, et al. Structural study of sol–gel silicate glasses by IR and Raman spectroscopies[J]. J Non-Cryst Solids, 2009, 355: 475−480.

[27] ALI M A, REN J, LIU X, et al. Understanding enhanced upconversion luminescence in oxyfluoride glass-ceramics based on local structure characterizations and molecular dynamics simulations[J]. J Phys Chem C, 2017, 121: 15384−15391.

[28] ALI M A, REN J, LIU X, et al. Effect of ligand field symmetry on upconversion luminescence in heat treated $LaBGeO_5$:Yb^{3+},Er^{3+} glass[J]. J Am Ceram Soc, 2018, 101: 4387−4396.

[29] FRÉDÉRIC A, OLIVIER V, SOPHIE S, et al. Effect of temperature and thermal history on borosilicate glass structure[J]. Phys Rev B, 2012, 85: 054110.

[30] NESBITT H W, BANCROFT G M, HENDERSON G S, et al.

Bridging, non-bridging and free (O^{2-}) oxygen in Na_2O-SiO_2 glasses: an X-ray photoelectron spectroscopic (XPS) and nuclear magnetic resonance (NMR) study[J]. J Non-Cryst Solids, 2011, 357: 170–180.

[31] MIURA Y, KUSANO H, NANBA T, et al. X-ray photoelectron spectroscopy of sodium borosilicate glasses[J]. J Non-Cryst Solids, 2001, 290: 1–14.

[32] DAI X, BAI J, LI D, et al. Experimental and theoretical investigation on relationship between structures of coal ash and its fusibility for Al_2O_3-SiO_2-CaO-FeO system[J]. J Fuel Chem Technol, 2019, 47: 641–648.

[33] TODEA M, VANEA E, BRAN S, et al. XPS analysis of aluminosilicate microspheres bioactivity tested *in vitro*[J]. Appl Surf Sci, 2013, 270: 777–783.

[34] JANG H K, CHUNG Y D, WHANGBO S W, et al. Effects of chemical etching with nitric acid on glass surfaces[J]. J Vac Sci Technol A, 2001, 19: 267–274.

[35] KADEN W E, POMP S, STERRER M, et al. Insights into silica bilayer hydroxylation and dissolution[J]. Top Catal, 2017, 60: 471–480.

[36] LIU N, HUANG X, DUBOWSKI J J. Selective area in situ conversion of Si(001) hydrophobic to hydrophilic surface by excimer laser irradiation in hydrogen peroxide[J]. J Phys D: Appl Phys, 2014, 47: 385106.

[37] JANG H K, CHUNG Y D, WHANGBO S W, et al. Effects of chemical etching with sulfuric acid on glass surface[J]. J Vac Sci Technol A, 2000, 18: 401–404.